RSC Advances

ROYAL SOCIETY OF CHEMISTRY

www.rsc.org/advances

Cite this: DOI: 10.1039/c0xx00000x

www.rsc.org/xxxxxx

ARTICLE TYPE

Effective regulation of micro-structure of thick P3HT:$PC_{71}BM$ film by the incorporation of ethyl benzenecarboxylate in toluene solution

Wenfei Shen[a†], Manjun Xiao[b†], Jianguo Tang*[a], Xinzhi Wang[a], Weichao Chen*[b], Renqiang Yang*[b], Xichang Bao[b], Yao Wang[a], Jiqing Jiao[a], Linjun Huang[a], Jixian Liu[a], Wei Wang[a], Laurence A. Belfiore*[a,c]

Received (in XXX, XXX) Xth XXXXXXXXX 20XX, Accepted Xth XXXXXXXXX 20XX
DOI: 10.1039/b000000x

In this work, ethyl benzenecarboxylate (EB) was creatively selected as the additive in the blend of poly(3-hexylthiophene)/ phenyl-C71-butyric acid methyl ester (P3HT/$PC_{71}BM$) in non-halogenated solvent toluene (TL). With the optimized incorporating concentration of EB (i.e. 2vol%) in toluene, the great power conversion efficiency (PCE) enhancement of 4.11% was achieved without thermal annealing, while a maximum PCE of 4.82% with thermal annealing was achieved at the same conditions. According to our systematical characterization results, we can conclude that we are successful to regulate micro-structures including phase separation, domain sizes of P3HT or $PC_{71}BM$ and the crystallinity of P3HT by incorporating 2vol% EB in TL solution. The effective of EB as the TL additive in P3HT/$PC_{71}BM$ can be interpreted based on its Hansen solubility parameters (HSPs) and its high boiling point.

1 Introduction

Bulk-heterojunction (BHJ) polymer solar cells (PSCs) have gained tremendous attention in the last ten years due to their advantages of low cost, lightweight, and flexibility compared to the inorganic semiconductor solar cells[1, 2]. Over 10% power conversion efficiencies (PCE) of PSCs have been achieved by using novel low band-gap semiconductor polymers[3] or applying advanced architectures[4, 5], which is much close to the PCE value that PSCs commercialization needed[6]. However, many disadvantages in present fabrication process of PSCs will restrict their commercialization, especially, the utilizing of halogenated organic solvents such as chloroform (CF), chlorobenzene (CB), and ortho-dichlorobenzene (o-DCB) which are very toxic organic solvents, that will undermine human's health and ruin the environment in the fabricating process of future commercialized PSCs[7, 8]. Hence, it is of crucial meaningful to search environmentally friendly solvent to replace the toxic halogenated solvents.

The spontaneous interpenetrating network structure formed in the drying process of solvents, therefore the choice of processing solvent has a notable impact on the resulting microstructure and thus on the photovoltaic performance. At the very beginning of studying PSCs, researchers tried to utilize toluene and xylene which have been widely used as the processing solvents of polymer light-emitting diodes (PLEDs)[9] to fabricate PSCs[10], however, the results demonstrated that the PCE of devices fabricated with CB was 2.6 times higher than that of devices fabricated with toluene[11], and the photovoltaic performance of devices fabricated with o-DCB were much better than that of devices fabricated with xylene[10]. Besides, some other papers[12-15] also demonstrated that utilizing only one single kind of non-halogenated solvent can not achieve a good photovoltaic performance as much as that of devices fabricated with halogenated solvents.

It has been well known that blends solvents offer the possibility to tailor the parameters of solvents such as solubility, boiling point, viscosity etc[16-18], therefore, utilizing non-halogenated blend solvents or additives in non-halogenated solvents as the processing solvents of PSCs maybe an effective method to achieve good photovoltaic performances. Alex K.-Y. Jen et al. reported high-efficiency PSCs based on PBDT-DNT/$PC_{71}BM$ with PCE >6% using xylene as the host processing solvent and 2.5% 1,2-dimethylnaphthalene (1,2-DMN) as the additive[19], in addition, they reported a PCE >7% for the PSCs based on PIDTT-DFBT/$PC_{71}BM$ with 1,2,4-trimethylbenzene (1,2,4-TMB) as the host processing solvent and 2.5% 1,2-DMN as the additive[8]. Maojie Zhang et al.[13] used the non-halogenated solvent as processing solvent and N-methyl pyrrolidone (NMP) as solvent additive achieving a 6.6% PCE of PSCs based on P3HT/ICBA.

In this work, we utilized EB as the additive of the blend of P3HT/$PC_{71}BM$ in non-halogenated solvent toluene. We demonstrated the reasons that EB was selected by the Hansen solubility parameters (HSPs)[20] of related materials. The optimized doping concentration of EB additive in toluene was 2%, and with this doping concentration we demonstrated a PCE of 4.11% without thermal annealing and a maximum PCE of 4.82% with thermal annealing. UV-Vis spectra, XRD, AFM and TEM characterization results indicated that better phase separation, larger P3HT or $PC_{71}BM$ domains and larger crystalinity of P3HT were formed in the films casted from toluene solutions with EB additive.

2 The choice of solvent additive

The addition of small amount of high boiling point additive to the host processing solvent can significantly improve the phase separation of interpenetrating network, which can be ascribed to the differential solubility of additive and host solvent for polymer donor or fullerene derivative acceptor, and the longer drying time for bigger crystallization[16]. As has been published[13, 15, 21], the solvent additives have a great effect on the fullerene solubility when they were incorporated into the non-halogenated solvents. For instance, the solubility of $PC_{71}BM$ in o-xylene can be greatly enhanced by the addition of 2.5 vol% 1-methylanphthalene (1-MN)[8]. This phenomenon can be expounded by the Hansen solubility parameters (HSPs), which were firstly introduced by Hildebrand and Scott to describe and predict the solubility behavior of organic semiconductors. The Hildebrand parameter δ that indicates the miscibility of the components in a blended solution was defined as the square root of the cohesion energy density as shown in Eqs. (1), where E is the energy change of the evaporation and V is the molar volume.

$$\delta = \sqrt{E/V} \qquad (1)$$

$$\delta^2 = \delta_D^2 + \delta_P^2 + \delta_H^2 \qquad (2)$$

The Hildebrand parameter is mainly determined by 3 factors as shown in Eqs (2), which are atomic dispersive interactions (δ_D), permanent dipole interactions (δ_P), and molecular hydrogen bonding interactions (δ_H), respectively. The HSPs parameters of solvent and solute can be plotted in a 3-dimentional coordinate system with δ_D, δ_P and δ_H as X, Y and Z axis, respectively. Therefore, the solubility of a solute in various solvents can be demonstrated by the Hansen sphere, where the HSP plot of the solute is located at the center of the sphere and the interaction radius R_o spanning the regime within which the solute is dissolved. The distance between the HSPs parameters of solvent and solute is defined as R_a, as represented in Eqs. (3), in which the 1 and 2 represent the solute and solvent, respectively.

$$R_a^2 = 4(\delta_{D1} - \delta_{D2})^2 + (\delta_{P1} - \delta_{P2})^2 + (\delta_{H1} - \delta_{H2})^2 \qquad (3)$$

The ratio of R_a and R_o defines the relative energy difference (RED), which can be used to estimate the solubility of a solute in a particular solvent. For instance, the solubility of a solvent for a solute is high when the RED<1, a solute in a solvent is partially dissolved when RED=1, and a solute in a solvent is insoluble when the RED>1[8, 22].

It can be found in reference[20] that the δ_D, δ_P and δ_H of toluene are 18.0, 1.4 and 2.0, respectively, whereas, the HSPs parameters of $PC_{71}BM$ are 20.2, 5.4 and 4.5, respectively[23]. All the HSPs parameters of toluene are located far away from that of $PC_{71}BM$, which indicates a bad solubility of $PC_{71}BM$ in toluene. To improve the morphology of the active layers that casted from the non-halogenated solvents, Alex K.-Y. Jen et al.[8] incorporated 2.5 vol% 1,2-DMN additive to the o-xylene. They found a much finer D/A separation in the BHJ films that casted from o-xylene solution with 2.5 vol% 1,2-DMN, which is very similar to that of BHJ films casted from o-DCB solutions. They ascribed the better morphology to the incorporation of 1,2-DMN that increased δ_D and δ_H of the solvents, in addition, the increased δ_D and δ_H lead to a decreased RED and better miscibility with $PC_{71}BM$. Inspired by this concept, we found that the δ_P and δ_H of EB are 6.2 and 6.0, respectively, which are relatively high and can be as the additive to increase the δ_P and δ_H values in toluene blend solution. The Hansen solubility parameters diagram of P3HT, $PC_{71}BM$ and related solvents is shown in Fig. 1, and detailed HSPs parameters of P3HT, $PC_{71}BM$ toluene and EB are summarized in Table 1. After carefully calculations, we got that the RED values of P3HT in toluene and EB are 0.75 and 1.25, respectively, and the RED values of $PC_{71}BM$ in toluene and EB are 0.77 and 0.58, respectively. This results demonstrate that toluene is a can dissolve P3HT and $PC_{71}BM$, comparatively speaking, EB is a bad solvent for P3HT and a good solvent for $PC_{71}BM$. Based on these characteristics, small amount of EB incorporation in toluene can improve the P3HT selectively aggregation, which is propitious to phase separation. Hence through control the incorporation concentration, we can effectively regulate the domain size of every phase. On the other hand, the boiling point of EB is 212.6 ℃, which is much bigger than that of TL (110.6 ℃). The incorporation of EB will increase the drying time of P3HT:$PC_{71}BM$ film, which will benefit the self-assemble of P3HT and the aggregation of $PC_{71}BM$. Besides, it is worth to note that EB is micro-poisonous to humans, and it exists naturally in peach, pineapple and black tea. Therefore, EB is a kind of environment-friendly additive which is not harmful to the humans' health and the environment. To conclude, EB is very suitable as the additive of P3HT:$PC_{71}BM$ toluene solution.

Table 1 The HSP parameters of solvents and materials.

Material/Solvents	HSPs [$MPa^{1/2}$]				RED with	
	δ_D	δ_P	δ_H	R_o	P3HT	$PC_{71}BM$
P3HT	19.05	3.3	2.8	3.9		
$PC_{71}BM$	20.2	5.4	4.5	8.4		
Toluene	18.0	1.4	2.0		0.75	0.77
EB	17.9	6.2	6.0		1.25	0.58

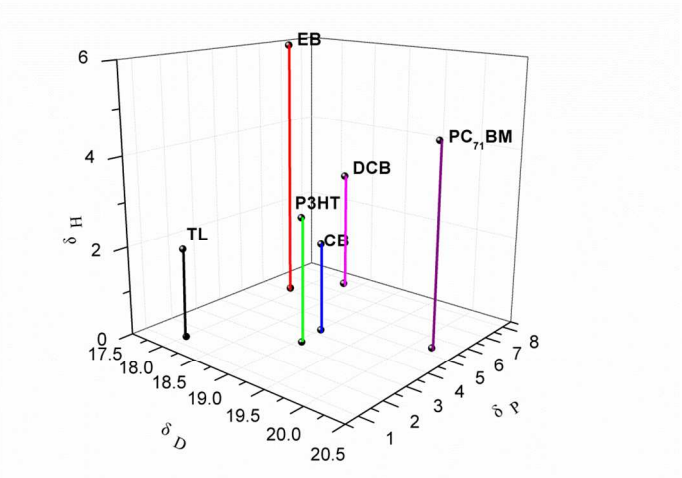

Fig. 1 The HSP parameters diagrams of solvents and materials related in this paper.

3 Experimental

3.1 Fabrication of PSCs

In this work, poly(3-hexylthiophene) (P3HT, 98%

regioregularity, Luminescence Ch) and phenyl-C71-butyric acid methyl ester (PC71BM, 99.5%, American Dye Sources Inc) were selected as photovoltaic materials. The device structure of polymer solar cells is shown as the following module: Glass/ITO/poly(3,4-ethyl-enedioxythiophene): poly(styrenesulfonate) (PEDOT:PSS)/P3HT:PC71BM/Ca/Al [6]. And Fig. 2 shows the schematic diagram of PSCs. The details of fabrication processes are shown as follows: ITO-coated glass substrates with a nominal sheet resistance of 15 Ω/sq were ultrasonically cleaned with detergent, de-ionized water, acetone and iso-propyl alcohol for 20 min in each round, and subsequently dried in an oven at 110℃. The substrates were treated in a Plasma cleaning instrument (Plasmon Preen II-862, Mycro Co.) for 6 min prior to the deposition of the hole transport materials. The PEDOT:PSS solution (Clevios PVP Al4083, HC Starck) was spin-coated at a speed of 4000 rpm for 30 s to form a hole transport layer and then annealed at 150℃ for 20 min. The thickness of the PEDOT:PSS film was about 40nm. To optimize the concentration effect of EB in the toluene solution, 1 vol%, 2 vol% and 3vol% of EB was added to P3HT:PC_{71}BM (1:1) toluene solution of 36 mg/ml. The blend solution was fully mixed before spin-coating. The substrates with PEDOT:PSS and blend solutions were then transferred into a nitrogen-filled glove box, and the P3HT:PCBM (1:1) toluene solutions were spin-coated on PEDOT:PSS layer at 600 rpm for 40 seconds to form ~330 nm thick active layers. The device fabrication parameters were optimized prior to this preparation of PSC. The fabricated PSC active layer subjected to thermal annealing at 160℃ for 10 min if needed. At last, Ca/Al electrodes were thermally evaporated onto the active layer with a thickness of 5 nm and 100 nm respectively, to form a cathode, at a vacuum (≤ 10-6 Torr) condition, and the active layer area of the device was 0.1 cm^2 defined by a shadow mask for all the solar cell devices discussed in this work[24].

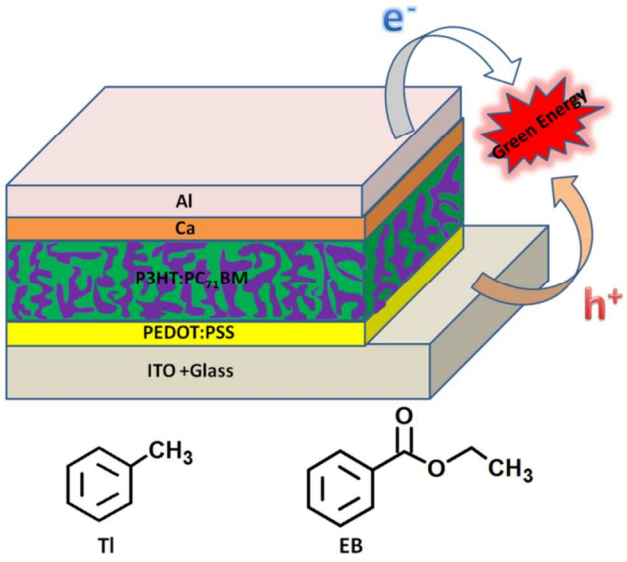

Fig. 2 The schematic diagram of the PSC structure, and the structural formulas of TL and EB.

To investigate the hole carrier mobility of P3HT:PC_{71}BM films that casted from toluene solution and toluene solutions with EB, we fabricated devices that can only transport holes, of which the structure is shown as following: ITO/PEDOT:PSS/P3HT:PC_{71}BM/Au. The charge carrier mobility of the devices were studied by the method of trap-free-space-charge-limited-current (SCLC)[12]. All the fabrication processes before evaporating metallic electrode were same with that of fabricating the devices of PSCs, the only difference was that the evaporated electrode is Au electrode.

3.2 Characterization

The current density-voltage (J-V) characteristics were measured under AM 1.5 solar illumination at an intensity of 100 mW/cm^2 with Newport solar simulator by a Keithley 2420 source measurement N_2 filled glove box. The external quantum efficiencies (EQE) of PSCs were analyzed using a certified Newport incident photon conversion efficiency (IPCE) measurement system. The UV-Vis absorption spectra of pristine P3HT:PC_{71}BM film and P3HT:PC_{71}BM films that casted from toluene solution and toluene solutions with EB were taken on a Varian Cary 50 UV-Vis spectrometer. The thickness of P3HT:PC_{71}BM films were acquired using a Veeco Dektak 150 surface profiler. The X-ray diffraction (XRD) spectra were taken by a Mac Science, equipped with Cu Kα source. 2-D X-ray scattering in grazing incidence geometry (GIWAXS) measurement was performed by Shanghai Synchrotron Radiation facility. Atomic force microscopy (AFM) measurements were carried out on an Agilent 5400 AFM at ambient temperature. The transmission electron microscopy (TEM) images of P3HT: PC_{71}BM film and P3HT:PC_{71}BM films that casted from toluene solution with EB were obtained on a JEM-2000 Ex.

4. Results and discussion

In order to evaluate the effect of EB in toluene, we fabricated devices with P3HT:PC_{71}BM casted from toluene solutions with 0 vol%, 1 vol%, 2vol% and 3 vol% EB. The J-V cures of these devices are shown in Fig. 3, and the detail photovoltaic parameters are summarized in Table 2. The device that without EB additive and thermal annealing shows a poor photovoltaic performance, with a low short circuit current density (Jsc) of 2.72 mA/cm^2 and a low fill factor of 35.65%, in addition, the Voc is distinctly higher than that of device with EB additive. All of these representations can be ascribed to the unavailable interpenetrating network of P3HT:PC_{71}BM. It can be easily found that the photovoltaic performances of devices that with EB additive is obviously better than that of device without EB additive. For instance, the Jsc and FF are greatly improved and therefore the PCEs of devices are greatly enhanced. With the incorporation of 2 vol% EB in toluene, we can get a best photovoltaic performance (PCE=4.11%) of device that without annealing. It is worth to note that with the increasing of EB concentration, the Voc of the devices is decreasing. Similar changes in Voc have been reported by Yang Yang .etc[16] for P3HT:PC_{71}BM devices decreased after the treatment of solvent annealing, and they ascribed the decrease of Voc to improved vertical phase segregation and the upward-shift HOMO level of P3HT when its aggregation enlarged. Hence, it is reasonable to consider that the incorporation of EB in toluene improved the phase separation of

P3HT:$PC_{71}BM$ even without thermal annealing. In addition, the photovoltaic performance of devices that fabricated with 2 vol% EB in toluene can be further improved to a maximum PCE of 4.82%, with the Jsc and FF reaching to maximum values of 11.48 mA/cm^2 and 69.97%, respectively.

Table 2 The photovoltaic parameters of devices.

	Voc (V)	Jsc (mA/cm^2)	FF (%)	PCE (%)
0	0.82	2.72	35.65	0.80
1	0.61	9.99	56.03	3.41
2	0.56	11.22	65.42	4.11
3	0.54	11.19	63.92	3.86
0 anneal	0.61	10.64	62.35	4.05
2 anneal	0.60	11.48	69.97	4.82

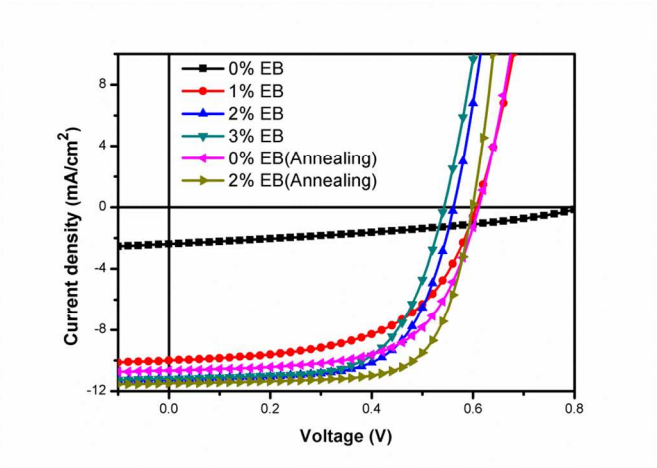

Fig. 3 The J-V curves of P3HT:$PC_{71}BM$ devices with different EB ratio.

External quantum efficiency (EQE) can verify the better photovoltaic performances of PSCs. Based on this concept, the EQE value reaches to 100% when all incident photons generate electron-hole excitons. However, EQE value used to be less than 100% due to the reflection of incident light, weak absorption of photo-active materials and the recombination of electrons and holes[24]. The EQE spectra of various devices are shown in Fig. 4. From the EQE spectra, we can see that even without thermal annealing the EQE intensities can be greatly enhanced by incorporating EB additive. And after thermal annealing, the devices with 2% EB additive shows a maximum EQE value which is in accordance with its maximum photovoltaic performance. All of the results are corresponding to that of device photovoltaic performances.

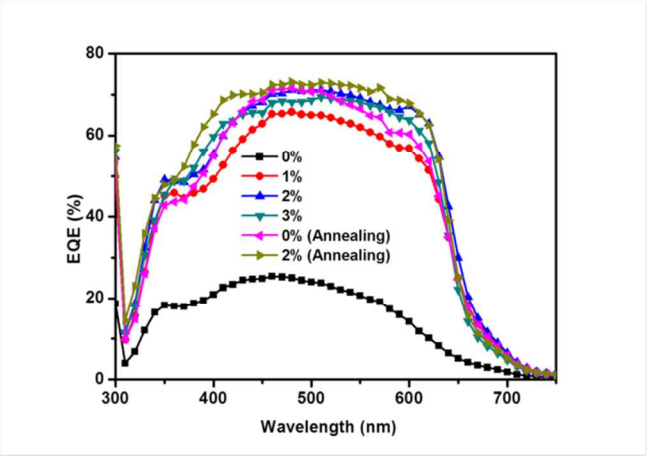

Fig. 4 The EQE spectra of P3HT:$PC_{71}BM$ devices with different EB ratio.

In order to uncover the reasons that caused the photovoltaic performances discrepancies of the devices that casted from toluene solutions with or without EB additive, we did the absorption characterization of the P3HT:$PC_{71}BM$ films, and the results are shown in Fig. 5a. It is easy to see that there are significant red shifts in absorption spectra of P3HT:$PC_{71}BM$ films that casted from toluene solutions with EB additive, compared with that of P3HT:$PC_{71}BM$ film casted from pure toluene solution. It is worth to note that there are three distinct characteristic absorption peaks in the absorption spectra with EB incorporation ratio >2%, which are a peak at ~520 nm, and two shoulders at ~550 nm and ~610 nm, respectively. The peak at 520 nm is corresponding to the π-π^* electron transition, and the other two shoulder peaks are ~~a~~ manifestation of strong interchain-interlayer interaction or high crystallinity of P3HT. Therefore, all of these results of the absorption spectra demonstrate an enhanced π-π stacking of the P3HT by incorporating EB into the toluene solutions.

To validate that it is due to the enhanced crystallinity of P3HT that causes the red shifts of the absorption spectra, we took the XRD characterizations on the films that casted from different toluene solutions with various EB ratios, and the results are shown in Fig. 5b. The diffraction peak of $2\theta \approx 5.5°$is the characteristic diffraction peak of P3HT crystal, which is corresponding to the (100) lattice plane of P3HT[12]. As we can see from the XRD spectra, all of the spectra of the films show strong diffraction peak at $2\theta \approx 5.5°$, but the intensity of the films increase with increasing of the EB incorporation ratio. To eliminate the possible influence of film thickness on the XRD diffraction intensity, we measured the films thicknesses and found no big differences as 325 nm, 330 nm, 338 nm and 342 nm, respectively. In addition, there are small peaks at $2\theta \approx 11°$ in the spectra of films with EB additives which are corresponding to the (200) lattice plane of P3HT, the emerging of the (200) lattice plane of P3HT indicates a large crystallinity of P3HT. So, it can be believed that the incorporation of EB can increase the crystallinity of P3HT.

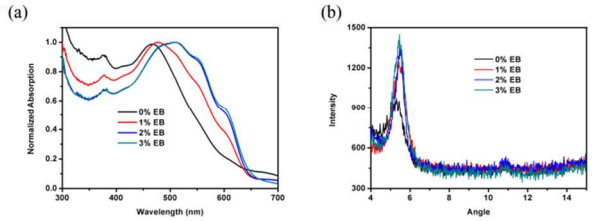

Fig. 5 (a) the absorption spectra of P3HT:$PC_{71}BM$ films that casted from toluene solutions with different EB ratio, (b) the XRD curves of P3HT:$PC_{71}BM$ films that casted from toluene solutions with different EB ratio.

To further understand the development of the crystal structure of P3HT and PCBM during the film-processing process, we take 2-D X-ray scattering in grazing incidence geometry (GIWAXS) measurement[16, 25]. The measurements were taken with the X-ray incident angle within the characteristic angles for total angle reflection of P3HT and PCBM but below that of Si substrate, which can probe the molecular ordering of entire thickness of active layer. The packing along the side chains of the P3HT crystal is denoted as the *a*-axis, (h00), and the π - π stacking direction within P3HT crystal is denoted as the *b*-axis, (0k0). From the GIWAXS results (Fig. 6), we can see that the addition of EB in toluene solution greatly increase the diffraction intensity (in the range of 0-5 nm^{-1}) of P3HT, which indicated that the crystallinity of P3HT is greatly enhanced. After treating with annealing process, the P3HT:PCBM film processed without EB showed higher diffraction intensity (~0-7 nm^{-1}), which corresponding to higher crytallinity of (100) and (200). However, the P3HT:PCBM film processed with 2% EB showed no diffraction intensity difference after annealing treatment. Besides, the diffraction intensity of the P3HT:PCBM film processed without EB was obvious lower than that of P3HT:PCBM film processed with 2% EB even after thermal annealing. Hence, it can be believed that the micro-structure regulation effect of EB can not be achieved by thermal annealing.

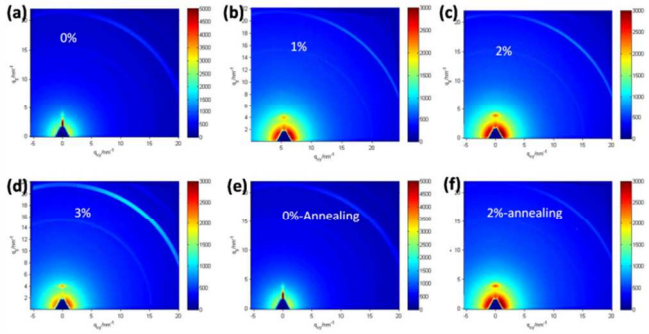

Fig. 6 2-D GIWAXS results of P3HT:PCBM processed with different amount of EB(a-d), and with thermal annealing treatment(e-f).

Previous studies showed that small amounts of additives still have great influence on the morphology of the films that formed. So we took AFM characterization to study the morphology changes of the P3HT:$PC_{71}BM$ that casted from toluene solutions with different EB additive ratios. Fig. 7 shows the AFM topographic images of the films. From Fig. 7, we can see that the P3HT:$PC_{71}BM$ film without EB additive shows a very smooth surface with a root mean square roughness (RMS) of 0.36 nm, and the films casted from solutions with EB additive show greatly enhanced RMS value, which are 2.2 nm, 8.9 nm and 9.2 nm, respectively. Larger roughness demonstrated larger donor/acceptor domain size, which means better donor/accepter interpenetrating network[13]. Therefore, we can believe that the better interpenetrating network benefits the extraction of holes and electrons. After carefully analysis, we ascribe the greatly enhanced RMS values to the enhanced phase separation that caused by the incorporation of EB. For instance, comparing with toluene, EB is a poor solvent for P3HT and a good solvent for $PC_{71}BM$. So small amounts of EB incorporation will lead to the aggregation of P3HT, which will good for the phase separation. However, only appropriate phase separation is needed for the relatively short excitons diffusion length (<20 nm). Excess EB additive (3%) will lead to enlarged phase separation which is not benefit the excitons diffusing to the interface of donor material and acceptor material, and thus will decrease the photovoltaic performance.

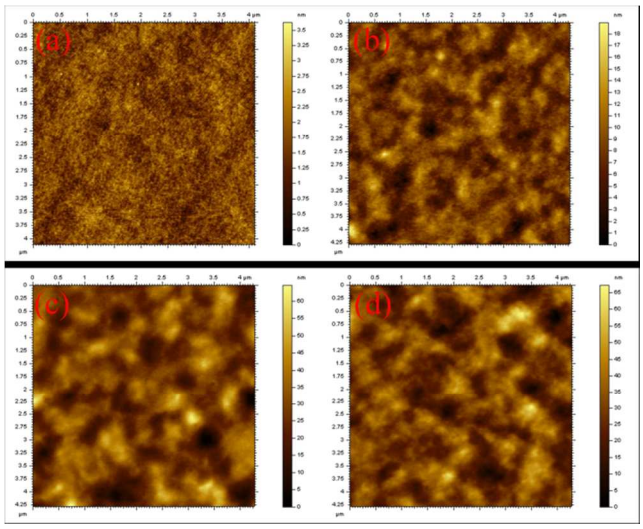

Fig. 7 The AFM images of P3HT:$PC_{71}BM$ films that casted from toluene solutions with (a) 0% EB, (b) 1% EB, (c) 2% EB and (d) 3% EB.

To intuitively demonstrate the phase separation differences between films that casted from toluene solution with or without EB additive, we took the TEM characterization of them. Fig. 8 shows the TEM images of films that casted from toluene solution without EB and with 2% EB. From the results, we can see that better interpenetrating network is formed after incorporating 2% EB additive, which is caused by its poor solubility for P3HT and good solubility for $PC_{71}BM$. Fig. 8a demonstrated a intensively mixed P3HT:$PC_{71}BM$ film that very small P3HT or $PC_{71}BM$ domains were formed, which goes against the transport of charge carriers. Whereas, there were instinct P3HT or $PC_{71}BM$ rich domains formed as shown in Fig. 8b, which will definitely improve the charge carrier transportation and prevent the unfavorable electron-hole recombination. However, as we have mention above, only appropriate domain size is needed for a balance of excitons diffusion and charge carrier transportation, so only appropriate EB doping concentration is needed.

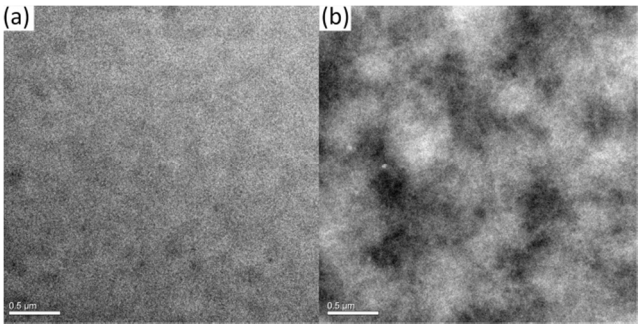

Fig. 8 The TEM images of P3HT:$PC_{71}BM$ films that casted from toluene solutions with (a) 0% EB and (b) 2% EB.

Charge carrier mobility is mainly depends on the crystallinity of P3HT and the domain size of $PC_{71}BM$, hence, according to the results of XRD and TEM, we speculated that the charge carrier mobility of the P3HT:$PC_{71}BM$ films that casted from toluene solutions with EB additives are much larger than that of films casted from solutions without EB additives. To testify our speculations, we investigated the hole mobility of P3HT:$PC_{71}BM$ films by the method of trap-free-space-charge-limited-current (SCLC). The J-V curves of the devices with the structure of ITO/PEDOT:PSS/P3HT:$PC_{71}BM$/Au were shown in Fig. 9 The calculated hole mobility (μ_h) of P3HT:$PC_{71}BM$ films that casted from toluene solutions with 0%, 1%, 2% and 3% EB additives are 1.26×10^{-7} $cm^2/V\cdot S$, 3.24×10^{-3} $cm^2/V\cdot S$, 4.80×10^{-3} $cm^2/V\cdot S$ and 3.91×10^{-3} $cm^2/V\cdot S$, respectively. From the results, we can see that the hole mobility of the films that casted from toluene solutions with EB additive improves more than 10000 times compared with that of film casted from pristine toluene solution. As we have mentioned above, we ascribe this enhancement to the improved crystallinity of P3HT and the enlarged P3HT of $PC_{71}BM$ domain sizes.

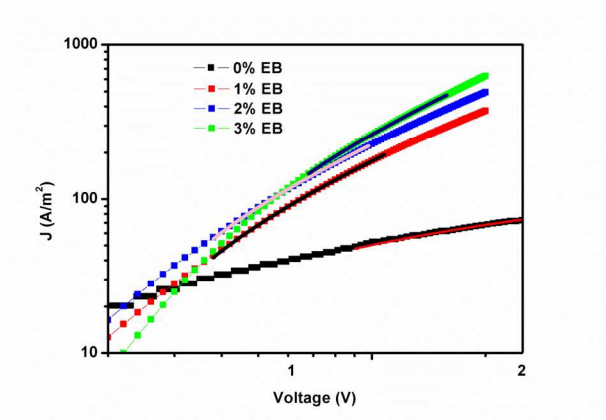

Fig. 9 The J-V curves for hole-only devices that fabricated with different EB ratios.

Conclusions

By studying the HSPs parameters of EB in P3HT:$PC_{71}BM$, we believe that EB can act as a processing additive in the toluene solution of P3HT:$PC_{71}BM$ for its poor P3HT solubility and good $PC_{71}BM$ solubility. After optimizing incorporation ratio, we demonstrated a 5.1 times enhanced PCE of PSCs even without thermal annealing, and a 4.82% PCE can be achieved after thermal annealing. By systematically analysis the results of absorption spectra, XRD spectra, AFM, TEM and SCLC, we concluded that the incorporation of EB in P3HT:$PC_{71}BM$ can increase the phase separation and the crystallinity of P3HT, and achieve an effective balance between excitons diffusion and charge carrier mobility.

Acknowledgements

This work was supported by: (1) The National One-Thousand Foreign Expert Program (WQ20123700111); (2) Natural Scientific Foundation of China, Grant #51273096; (3) Natural Scientific Foundation of China, Grant #51373081; (4) Natural Scientific Foundation of China, Grant #51473082; (5) Shandong Province Project: Tackle Key Problem in Key Technology, #2010GGX10327;

Notes and references

[a]*Institute of Hybrid Materials, the Growing Base for State Key Laboratory, Qingdao University, 308 Ningxia Road, Qingdao 266071, P. R. China*
[b]*Qingdao Institute of Bioenergy and Bioprocess Technology, Chinese Acadamy of Sciences, 189 Songling Road, Qingdao, 266101, P.R.China*
[c]*Department of Chemical and Biological Engineering, Colorado State University, Fort Collins, Colorado 80523, USA*
[†]*The authors contribute equally to this work.*
* *Corresponding author: Jianguo Tang (jianguotangde@hotmail.com)*
Tel. : +86 532 85951519 Fax: +86 532 85951519 ;
Weichao Chen (chenwc@qibebt.ac.cn)
Renqiang Yang (yangrq@qibebt.ac.cn)
Laurence A. Belfiore (belfiore@engr.colostate.edu)

1. A. J. Heeger, *Advanced Materials*, 2014, **26**, 10-28.
2. K. M. Coakley and M. D. McGehee, *Chemistry of Materials*, 2004, **16**, 4533-4542.
3. Z. He, C. Zhong, S. Su, M. Xu, H. Wu and Y. Cao, *Nature Photonics*, 2012, **6**, 591-595.
4. J. You, C. C. Chen, Z. Hong, K. Yoshimura, K. Ohya, R. Xu, S. Ye, J. Gao, G. Li and Y. Yang, *Advanced Materials*, 2013, **25**, 3973-3978.
5. J. You, L. Dou, K. Yoshimura, T. Kato, K. Ohya, T. Moriarty, K. Emery, C.-C. Chen, J. Gao and G. Li, *Nature communications*, 2013, **4**, 1446.
6. S. Gunes, H. Neugebauer and N. S. Sariciftci, *Chemical Reviews-Columbus*, 2007, **107**, 1324-1338.
7. L. Dou, J. You, Z. Hong, Z. Xu, G. Li, R. A. Street and Y. Yang, *Advanced Materials*, 2013, **25**, 6642-6671.
8. C.-C. Chueh, K. Yao, H.-L. Yip, C.-Y. Chang, Y.-X. Xu, K.-S. Chen, C.-Z. Li, P. Liu, F. Huang, Y. Chen, W.-C. Chen and A. K. Y. Jen, *Energy & Environmental Science*, 2013, **6**, 3241.
9. D. Acton and J. Barker, *Journal of Contaminant Hydrology*, 1992, **9**, 325-352.
10. Q. Pei, G. Yu, C. Zhang, Y. Yang and A. J. Heeger, *Science*, 1995, **269**, 1086-1088.
11. S. E. Shaheen, C. J. Brabec, N. S. Sariciftci, F. Padinger, T. Fromherz and J. C. Hummelen, *Applied Physics Letters*, 2001, **78**, 841-843.
12. M.-J. XIAO, W.-F. SHEN, J.-Y. WANG, L.-L. HAN, W.-C. CHEN, X.-C. BAO, R.-Q. YANG and W.-G. ZHU, Chin Phys. Lett, 2015, **2**, 028802.
13. X. Guo, M. Zhang, C. Cui, J. Hou and Y. Li, *ACS applied materials & interfaces*, 2014, **6**, 8190-8198.
14. Y. Chen, S. Zhang, Y. Wu and J. Hou, *Adv Mater*, 2014, **26**, 2744-2749, 2618.
15. B. R. Aïch, S. Beaupré, M. Leclerc and Y. Tao, *Organic Electronics*, 2014, **15**, 543-548.

16. G. Li, Y. Yao, H. Yang, V. Shrotriya, G. Yang and Y. Yang, *Advanced Functional Materials*, 2007, **17**, 1636-1644.
17. J. K. Park, C. Kim, B. Walker, T.-Q. Nguyen and J. H. Seo, *RSC Advances*, 2012, **2**, 2232-2234.
18. D. Wang, F. Zhang, L. Li, J. Yu, J. Wang, Q. An and W. Tang, *RSC Advances*, 2014, **4**, 48724-48733.
19. C.-C. Chueh, K. Yao, H.-L. Yip, C.-Y. Chang, Y.-X. Xu, K.-S. Chen, C.-Z. Li, P. Liu, F. Huang and Y. Chen, *Energy & Environmental Science*, 2013, **6**, 3241-3248.
20. C. M. Hansen, *Hansen solubility parameters: a user's handbook*, CRC press, 2007.
21. K.-S. Chen, H.-L. Yip, C. W. Schlenker, D. S. Ginger and A. K.-Y. Jen, *Organic Electronics*, 2012, **13**, 2870-2878.
22. F. Machui, S. Langner, X. Zhu, S. Abbott and C. J. Brabec, *Solar Energy Materials and Solar Cells*, 2012, **100**, 138-146.
23. B. Walker, A. Tamayo, D. T. Duong, X.-D. Dang, C. Kim, J. Granstrom and T.-Q. Nguyen, *Advanced Energy Materials*, 2011, **1**, 221-229.
24. W. Shen, J. Tang, R. Yang, H. Cong, X. Bao, Y. Wang, X. Wang, Z. Huang, J. Liu and L. Huang, *RSC Advances*, 2014, **4**, 4379-4386.
25. N. D. Treat, M. A. Brady, G. Smith, M. F. Toney, E. J. Kramer, C. J. Hawker and M. L. Chabinyc, *Advanced Energy Materials*, 2011, **1**, 82-89.